

Age-related effects on the association between alcohol use severity and resting-state fMRI: a rodent study comparing adolescent-onset with adult-onset drinking

Supplements

1.1 Boilerplate for preprocessing

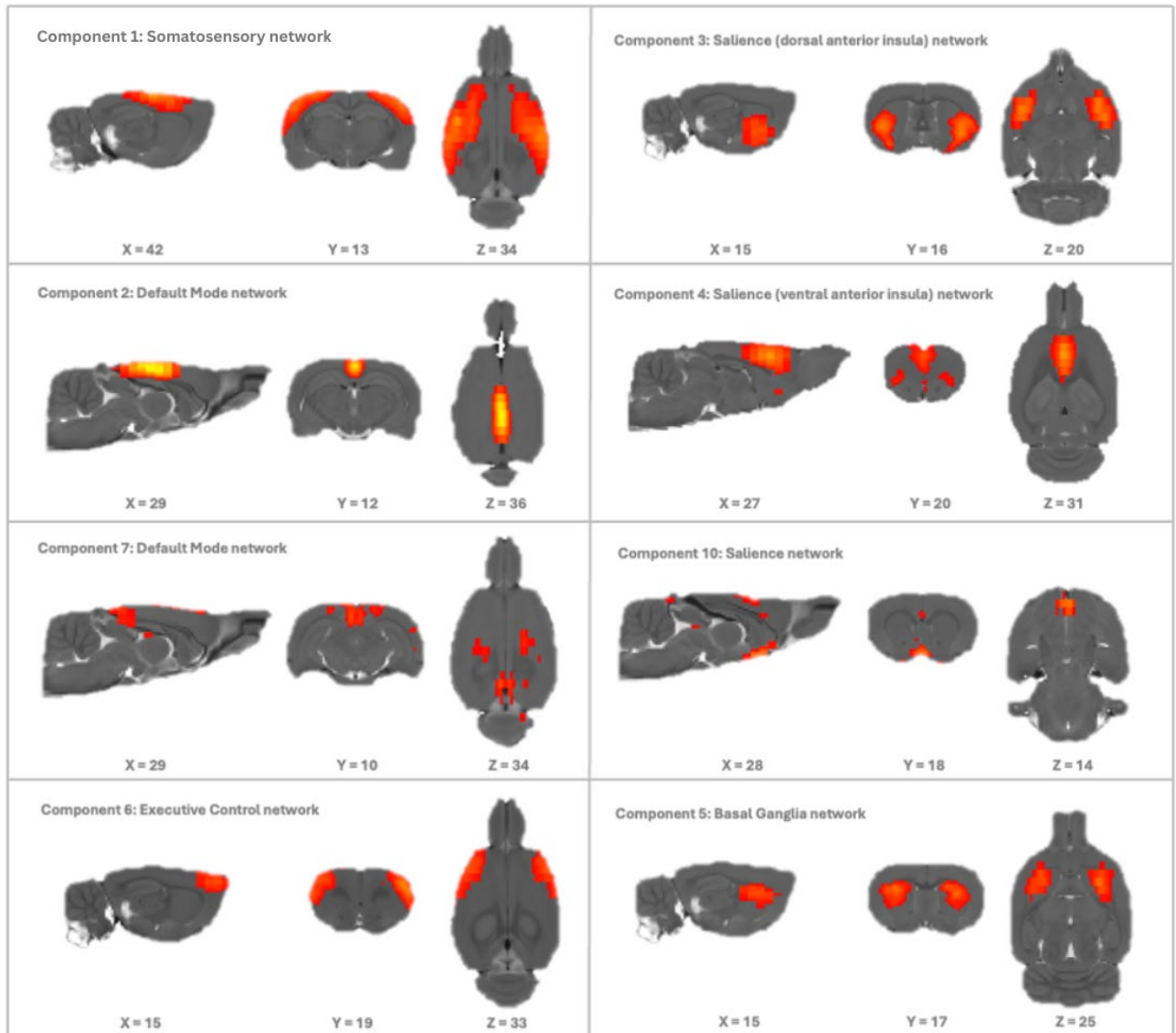
The preprocessing of fMRI images was conducted using the open-source RABIES software (<https://github.com/CoBrALab/RABIES>) (Desrosiers-Gregoire et al., n.d.). A volumetric EPI image was derived using a trimmed mean across the EPI frames, after an initial motion realignment step. Using this volumetric EPI as a target, the head motion parameters are estimated by realigning each EPI frame to the target using a rigid registration. To conduct common space alignment, structural images, which were acquired along the EPI scans, are initially corrected for inhomogeneities and then registered together to allow the alignment of different MRI acquisitions. This registration is conducted by generating an unbiased data-driven template through the iterative nonlinear registration of each image to the dataset consensus average, where the average gets updated at each iteration to provide an increasingly representative dataset template (https://github.com/CoBrALab/optimized_antsMultivariateTemplateConstruction) (Avants et al., 2011). The finalized template after the last iteration provides a representative alignment of each MRI session to a template that shares the effective acquisition properties of the dataset (shape, contrast), which makes it a stable registration target for cross-subject alignment. After aligning the MRI sessions, this newly-generated unbiased template is then itself registered, using a nonlinear registration, to an external reference atlas to provide both an anatomical segmentation and a common space comparable across studies defined from the provided reference atlas. To correct for EPI susceptibility distortions, the volumetric EPI is also subjected to inhomogeneity correction, and then registered using a nonlinear registration to the anatomical scan from the same MRI session, which allows to calculate the required geometrical transforms for recovering brain anatomy (Wang et al., 2017). Finally, after calculating the transformations required to correct for head motion and susceptibility distortions, transforms were concatenated into a single resampling operation (avoiding multiple resampling) which is applied at each EPI frame, generating the preprocessed EPI timeseries in native space (Esteban et al., n.d.). Preprocessed timeseries in common space are

also generated by further concatenating the transforms allowing resampling to the reference atlas.

1.2 Boiler plate for confound correction step

Confound correction was executed using the RABIES software (<https://github.com/CoBrALab/RABIES>) (Desrosiers-Gregoire et al., n.d.) on EPI timeseries resampled to commonspace. First, voxelwise detrending was applied to remove first-order drifts and the average image. Next, highpass filtering(0.01Hz) was applied using a 3rd-order Butterworth filter, and 30.0 seconds is removed at each edge of the timeseries to account for edge artefacts following filtering (Power et al., 2014). The removal of 30 seconds and the use of a 3rd order filter was selected based on the visualization of edge artefacts with simulated data. The nuisance regressors are also filtered to ensure orthogonality between the frequency filters and subsequent confound regression, which can otherwise re-introduce removed confounds (Lindquist et al., 2019) Selected nuisance regressors were then used for confound regression. More specifically, using ordinary least square regression, the 6 rigid motion parameters and the mean signal from the WM and CSF masks were modelled at each voxel and regressed from the data. To normalize variance, each image was separately scaled according to its total variance. Finally, a spatial Gaussian smoothing filter (`nilearn.image.smooth_img`)(Abraham et al., 2014) was applied at 0.3mm full-width at half maximum (FWHM).

1.3 Output from Group-ICA



References

- Abraham, A., Pedregosa, F., Eickenberg, M., Gervais, P., Mueller, A., Kossaifi, J., Gramfort, A., Thirion, B., & Varoquaux, G. (2014). Machine learning for neuroimaging with scikit-learn. *Frontiers in Neuroinformatics*, *8*(FEB). <https://doi.org/10.3389/fninf.2014.00014>
- Avants, B. B., Tustison, N. J., Song, G., Cook, P. A., Klein, A., & Gee, J. C. (2011). A reproducible evaluation of ANTs similarity metric performance in brain image registration. *NeuroImage*, *54*(3), 2033–2044. <https://doi.org/10.1016/j.neuroimage.2010.09.025>
- Desrosiers-Gregoire, G., Devenyi, G. A., Grandjean, J., & Chakravarty, M. M. (n.d.). *Rodent Automated Bold Improvement of EPI Sequences (RABIES): A standardized image processing and data quality platform for rodent fMRI*. <https://doi.org/10.1101/2022.08.20.504597>
- Esteban, O., Markiewicz, C. J., Blair, R. W., Moodie, C. A., Isik, A. I., Erramuzpe, A., Kent, J. D., Goncalves, M., Dupre, E., Snyder, M., Oya, H., Ghosh, S. S., Wright, J., Durnez, J., #1, R. A. P., & Gorgolewski #1, K. J. (n.d.). *FMRIPrep: a robust preprocessing pipeline for functional MRI*. <https://doi.org/10.6084/m9.figshare.6196994.v3>
- Lindquist, M. A., Geuter, S., Wager, T. D., & Caffo, B. S. (2019). Modular preprocessing pipelines can reintroduce artifacts into fMRI data. *Human Brain Mapping*, *40*(8), 2358–2376. <https://doi.org/10.1002/hbm.24528>
- Power, J. D., Mitra, A., Laumann, T. O., Snyder, A. Z., Schlaggar, B. L., & Petersen, S. E. (2014). Methods to detect, characterize, and remove motion artifact in resting state fMRI. *NeuroImage*, *84*, 320–341. <https://doi.org/10.1016/J.NEUROIMAGE.2013.08.048>
- Wang, S., Peterson, D. J., Gatenby, J. C., Li, W., Grabowski, T. J., & Madhyastha, T. M. (2017). Evaluation of field map and nonlinear registration methods for correction of susceptibility artifacts in diffusion MRI. *Frontiers in Neuroinformatics*, *11*. <https://doi.org/10.3389/fninf.2017.00017>